Relationship between the mean periods of wind-generated and infragravity waves: a sensitivity analysis

D. Mendes (1,2,3), A.A. Pires-Silva (1), J.P. Pinto (3) and A.B. Fortunato (2)

(1) CERIS, Instituto Superior Técnico, Universidade de Lisboa, Lisbon, Portugal. ddiogosm@gmail.com

(2) National Laboratory for Civil Engineering, Lisbon, Portugal.

(3) Hydrographic Institute, Lisbon, Portugal.

Abstract: A sensitivity analysis was performed on the mean infragravity wave period by varying five input parameters associated to short-waves. The mean infragravity wave period was estimated from the short-wave directional spectrum using a second-order wave theory.
The analysis was based on a sensitivity index and showed that the mean infragravity wave period is more sensitive to both the significant short wave height and the mean short wave period than to the water depth, the directional spreading coefficient and the JONSWAP peak-enhancement factor. The maximum value of the mean infragravity wave period obtained (60 s) indicates that larger mean infragravity wave periods might not be forced by the second-order wave theory, thereby depending on the bottom topography.

Key words: Infragravity waves, sensitivity analysis, second-order wave theory

1. INTRODUCTION

Infragravity waves (IGW) with periods between 25 s and 250 s often dominate the swash spectrum (Guza and Thornton, 1982). Following the mechanism proposed by Longuet-Higgins and Stewart (1962), these IGW are generated by nonlinear interactions between groups of wind-generated short-waves (SW) with periods between 4 s and 25 s. IGW generated by this mechanism are commonly referred as bound IGW.

Several dependencies of the significant IGW height (H_{ig}) are well established, such as the significant SW height (H_{sw}), the water depth (h) and the bottom slope (β). In general, H_{ig} increases with an increase in H_{sw} and a decrease in h. The growth rate of IGW is also larger over mild than over steep slopes because SW nonlinearities are stronger and occur in a large cross-shore length in the former.

Besides the above-mentioned dependencies, the relationship between the mean IGW period (T_{ig}) and the mean SW period (T_{sw}) remains unclear (Bertin *et al.*, 2018). As an example, while Bertin and Olabarrieta (2016) measured a T_{ig} of 60 s under narrow swell conditions characterized by a peak SW period (T_p) of 20 s, De Bakker *et al.* (2014) measured a T_{ig} of 200 s under broad sea conditions with a T_p of 7 s.

The aim of this study is to perform an analytical analysis on three IGW parameters by varying four parameters associated to SW and h. In particular, this study aims to understand based on a sensitivity index which SW parameters influence T_{ig} the most.

2. METHODOLOGY

1.1. Input and output parameters and sampling strategy

The sensitivity analysis performed in this study considered five input and three output parameters. The input parameters were H_{sw}, T_{sw}, h, the directional spreading parameter (s_{max}) and the peak-enhancement factor of the JONSWAP spectrum (γ). The output parameters were H_{ig}, T_{ig} and the IGW frequency bandwidth (ν_{ig}). The workflow is illustrated in Fig. 1.

The input dataset comprised 300 groups of five input parameters. The intervals of variation for H_{sw}, h, s_{max} and γ were respectively between 0.5 m and 6 m, 10 m and 100 m, 15 and 75, and 0 and 10. A uniform distribution was used to sample H_{sw}, h and s_{max}. A Gaussian distribution with a mean of 3.3 and a standard deviation of 0.8 (Ochi, 1998) was used to sample γ. In commonly observed sea-states, H_{sw} depends on T_{sw}. Therefore, we used a one-year time series records from the coastal buoy located in Leixões to estimate a relationship between both parameters. The following second-order polynomial relationship was established with a correlation coefficient of 0.69:

$$T_{sw} = -0.082H_{sw}^2 + 1.733H_{sw} + 7.746 \quad (1)$$

1.2. Directional short wave spectrum

The calculation of a directional SW spectrum largely followed Goda (2000). Therefore, the reader is referred to this textbook in order to fully understand the equations' numbering presented below.

A uni-directional JONSWAP-Goda type spectrum was calculated for each group of three input parameters associated to SW (H_{sw}, T_{sw} and γ) using Eq. (2.12) with a frequency resolution of 0.002 Hz and a high-frequency cut-off of 0.5 Hz.

A directional SW spectrum was computed following a cos^2 directional spreading function. First, we estimated s using Eq. (2.24) and s_{max}. Second, we calculated G_0 with Eq. (2.23). Third, we computed G with Eq. (2.21) for a directional interval between -180º and 180º. Finally, we obtained a directional SW spectrum with Eq. (2.19).

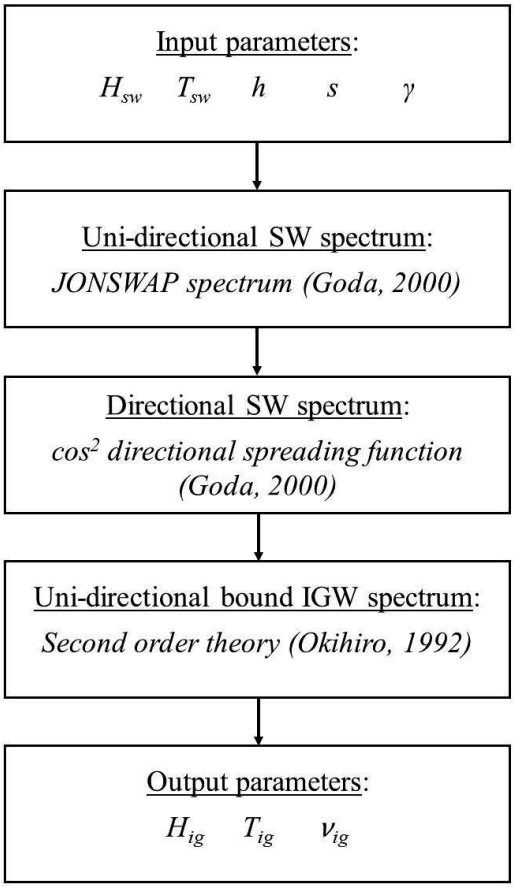

Fig. 1. Workflow of the methodology employed in this study.

Goda (2000) gave different values of s_{max} parameter based on the type of sea-state. As an example, local wind-generated waves (sea) are associated to a s_{max} of 10 while distant wind-generated waves (swell) display s_{max} values between 25 and 75. Consequently, we chose the s_{max} input parameter to follow a uniform distribution with a minimum value of 10 and a maximum value of 75.

1.3. Bound infragravity wave spectrum

The directional SW spectrum is used to estimate the uni-directional bound IGW spectrum following the formulation of Okihiro et al. (1992). This formulation makes use of the second-order wave theory. Lo and Dean (1995) showed that second-order wave theory is valid for a $H/L > 0.1$, where H is the SW height and L the wavelength. In shallower water depths this theory does not hold and the energy associated to the bound IGW spectrum will be overestimated. Therefore, we chose a minimum h of 10 m. The three output parameters were obtained from the spectral moments integration associated to the bound IGW spectrum. The integration limits were between 0.002 Hz and f_s ($f_s = 1/2T_{sw}$). ν_{ig} was calculated based on the formulation of Longuet-Higgins (1984). Again, we refer to Fig. 1 for a complete understanding of the procedure delineated above.

1.4. Sensitivity analysis

A sensitivity analysis (SA) was performed by using the input and output parameters for each of the 300 groups under study. The SA made use of the freely available SAFE toolbox (www.safetoolbox.info/). Details of the SAFE toolbox can be found in Pianosi *et al*. (2015). Here, we made use of a Regional Sensitivity Analysis (RSA) to estimate a sensitivity index.

The procedure used in the computation of the sensitivity index associated to the RSA will be briefly described in the following. The output parameter T_{ig} will be used as an example. First, a threshold value is chosen for T_{ig}. In our study, T_{ig} ranged between 25 s and 75 s and we chose 35 s for the threshold value. Second, the dataset associated to each input parameter was split in two sub-datasets: one associated to values of T_{ig} smaller than 35 s and the other with values of T_{ig} greater than 35 s. Third, the cumulative density function was calculated for each sub-dataset. Fourth, the maximum vertical distance between the cumulative density functions of each sub-dataset was used as a sensitivity index. By using this procedure, the sensitivity index displays values between 0 and 1. A value of 0 means that the output parameter is not sensitive to the input parameter. Note that there will be five sensitivity indexes (five input parameters) for each output parameter.

3. RESULTS AND DISCUSSION

The objective of this study is to improve the understanding of the dependencies associated to T_{ig}. Consequently, the results and discussion will only regard T_{ig}.

Fig. 2 shows the relationship between T_{ig} and each input parameter. A linear dependency is seen between T_{ig} and H_{sw} and T_{sw}. The values of the other input parameters are scattered for different values of T_{ig}.

Fig.2 also shows a maximum value of approximately 60 s for T_{ig}. A previous analysis by using a Pierson-Moskovitz instead of a JONSWAP-Goda type spectrum displayed similar results (not shown). Therefore, it seems that bound IGW are relatively short in period and the 200 s IGW periods observed

by De Bakker *et al*. (2014) might not be associated with bound waves, but rather with other types of IGW motions, such as edge waves.

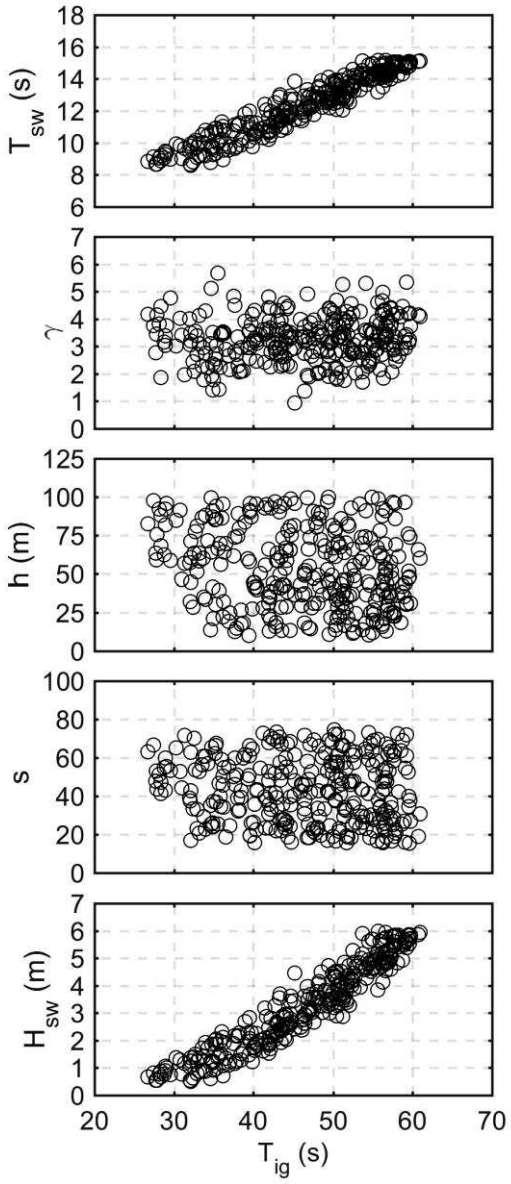

Fig. 2. Relationship between the mean infragravity wave period and the input parameter (from top to bottom) mean short wave period, JONSWAP peak-enhancement factor, water depth, maximum directional spreading coefficient and significant short wave height.

Fig. 3 displays the sensitivity index associated to T_{ig} for each input parameter. The T_{ig} is more sensitive to H_{sw} and T_{sw} than to the other parameters. We used a threshold value of 35 s for T_{ig} to make Fig. 3. We further analysed the results for a range of threshold values between 30 s and 50 s in 10 s intervals and the results did not change. Therefore, both H_{sw} and T_{sw} are the input parameters that influence T_{ig} the most.

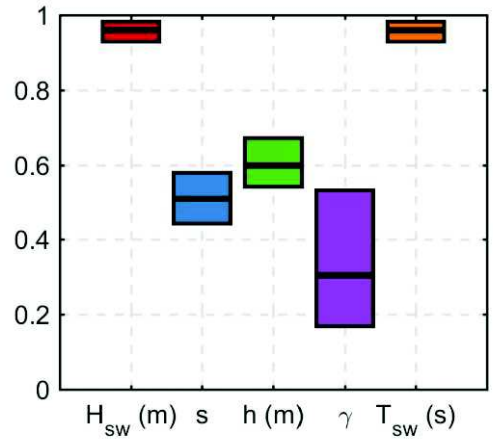

Fig. 3. Sensitivity index and upper and lower bounds of the sensitivity index after bootstrapping of the mean infragravity wave period associated to each input parameter.

Finally, Fig. 4 depicts a convergence plot for each input parameter to assess if 300 groups of input parameters are sufficient. Most of the input parameters seem to display a stable behaviour after approximately 240 groups. Consequently, 300 groups are adequate to perform this sensitivity analysis.

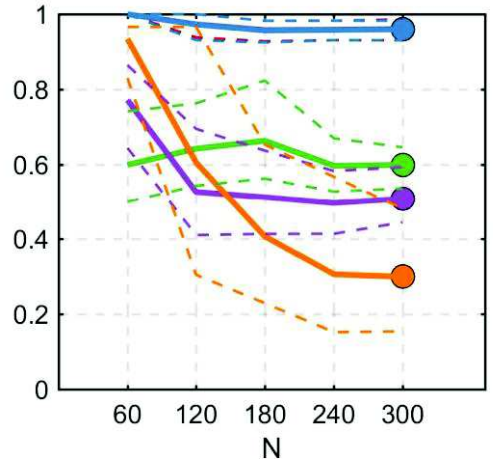

Fig. 4. Convergence associated to the sensitivity index of the mean infragravity wave period associated to each input parameter as a function of the number of input length. Orange, purple, green, blue and red lines indicate γ, s, h, H_{sw} and T_{sw}, respectively.

4. CONCLUSIONS

This study had its focus on a sensitivity analysis to improve the understanding between the mean IGW period and several SW parameters. From this sensitivity analysis, the parameters that most influence the mean IGW period are the significant SW height and the mean SW period. The maximum mean IGW period was 60 s by using a second-order wave theory. Therefore, larger IGW periods O(100 s) might be associated to other IGW motions not generated by this theory.

Acknowledgements

The first author acknowledges a PhD fellowship granted by Fundação para a Ciência e a Tecnologia (grant PD/BD/114463/2016).

REFERENCES

Bertin, X. and Olabarrieta, M. (2016). Relevance of infragravity waves in a wave-dominated inlet. *Journal of Geophysical Research: Oceans*, 121(8), 5418-5435.

Bertin, X. *et al.* (2018). Infragravity waves: from driving mechanisms to impacts. *Earth Science Reviews*, 177, 774-799.

De Bakker, A.T.M., Tissier, M.F.S., Ruessink, B.G. (2014). Shoreline dissipation of infragravity waves. *Continental Shelf Research*, 72, 73-82.

Goda, Y. (2000). *Random seas and design of maritime structures*. World Scientific. 443 pp.

Guza, R.T. and Thornton, E.B. (1982). Swash oscillations on a natural beach. *Journal of Geophysical Research: Oceans*, 87 (C1), 483-491.

Lo, J.M. and Dean, R.G. (1995). Long waves due to interactions beneath wave groups. *Journal of Waterway, Port, Coastal, and Ocean Engineering.* 121(6), 317-325.

Longuet-Higgins, M.S. (1984). Statistical properties of wave groups in a random sea state. *Philosophical Transactions of the Royal Society of London A*. 312, 219-250.

Longuet-Higgins, M.S. and Stewart, R.W. (1962). Radiation stress and mass transport in gravity waves, with application to 'surf beats'. *Journal of Fluid Mechanics*, 13, 481-504.

Ochi, M. (1998). *Ocean Waves: The Stochastic Approach*. Cambridge University Press. 332 pp.

Okihiro, M., Guza, R.T., Seymour, R.J. (1992). Bound infragravity waves. *Journal of Geophysical Research: Oceans*. 97(C7), 11453-11469.

Pianosi, F., Sarrazin, F., Wagener, T. (2015). A Matlab toolbox for Global Sensitivity Analysis. *Environmental Modelling & Software*, 70, 80-85.